

CONFIDENTIAL

Copy
RM H57E01

21

UNCLASSIFIED



3 1176 00092 5538

NACA

RESEARCH MEMORANDUM

FLIGHT MEASUREMENTS AND CALCULATIONS OF WING LOADS AND
LOAD DISTRIBUTIONS AT SUBSONIC, TRANSONIC, AND
SUPERSONIC SPEEDS

By Frank S. Malvestuto, Thomas V. Cooney,
and Earl R. Keener

High-Speed Flight Station
CLASSIFICATION CHANGED Edwards, Calif.

UNCLASSIFIED

LIBRARY COPY

JUL 10 1957

LANGLEY AERONAUTICAL LABORATORY
LIBRARY, NACA
LANGLEY FIELD, VIRGINIA

To

By authority of

TPH# 39 Date 1/12/61
CLASSIFIED DOCUMENT

This material contains information affecting the National Defense of the United States within the meaning of the espionage laws, Title 18, U.S.C., Secs. 793 and 794, the transmission or revelation of which in any manner to an unauthorized person is prohibited by law.

NATIONAL ADVISORY COMMITTEE FOR AERONAUTICS

WASHINGTON

July 2, 1957

CONFIDENTIAL

UNCLASSIFIED

NACA RM H57E01

UNCLASSIFIED

NATIONAL ADVISORY COMMITTEE FOR AERONAUTICS

RESEARCH MEMORANDUM

FLIGHT MEASUREMENTS AND CALCULATIONS OF WING LOADS AND
LOAD DISTRIBUTIONS AT SUBSONIC, TRANSONIC, AND
SUPERSONIC SPEEDSBy Frank S. Malvestuto, Thomas V. Cooney,
and Earl R. Keener

SUMMARY

Presented in this report is a summary of local and net angle-of-attack wing-panel loads measured in flight on six airplanes. In addition, a comparison of these loads measured in flight with calculations based on simple theory is presented.

INTRODUCTION

At the High-Speed Flight Station of the National Advisory Committee for Aeronautics, full-scale research in the fields of stability, performance, and loads is conducted with a variety of completely instrumented research and military-type airplanes.

In the present paper, the aerodynamic loads aspect of this flight research is considered. The presentation will involve a summary of local and net angle-of-attack wing-panel loads measured in flight on a variety of airplanes flown during the past 5 or 6 years. In addition, a preliminary comparison of these loads measured in flight and the corresponding loads calculated by simple theory is presented. The object of this comparison is to assess the ability of simple theoretical techniques to predict the flight-measured loads for a variety of configurations. Only a cursory comparison of the flight measurements with comparable wind-tunnel results has been made. In a general sense, the flight results verify the tunnel findings. For the convenience of the reader, a bibliography has been added.

Figure 1 depicts with plan-view outlines the airplanes to be discussed in this report. The wing panels are darkened to emphasize the fact that only the wing loads will be considered. An inspection of the individual sketches and geometric data shows that there is a good coverage of wing sweep, plan form, aspect ratio, and thickness. In addition, the X-1E wing has 2° positive incidence and the D-558-II wing has 3° of positive incidence. The free-stream Reynolds number for the flights of these airplanes varied from 1×10^6 to 6×10^6 per foot. The altitude varied from 25,000 feet to 65,000 feet.

UNCLASSIFIED

SYMBOLS

A	aspect ratio
b'	wing-panel span
b_f	flap span
c	chord
c_{av}	average chord
c_f	flap chord
c_n	section normal-force coefficient
C_N	net normal-force coefficient
C_{N_α}	variation of wing-panel normal-force coefficient with angle of attack
C_p	pressure coefficient
ΔC_p	pressure coefficient differential between upper and lower surfaces
H	altitude
i_w	wing incidence
M	free-stream Mach number
R_∞	free-stream Reynolds number
t	thickness
x	distance along x-axis
y	distance along y-axis
α	angle of attack
δ_e	elevon deflection
Λ_{LE}	leading-edge sweep

THEORIES CONSIDERED

A few preliminary remarks regarding the theories used for the wing-panel load calculations will be made. The wings are assumed to be rigid flat plates and of negligible thickness. In addition, the effect of the fuselage interference on the wing loads was approximated by assuming the fuselage to act as a perfect reflection plane located at the wing-fuselage juncture. On this basis, the wing load is predicted as the load on one panel of a symmetrical wing with its root chord coincident with the wing-fuselage juncture. It is realized that this approximation to the fuselage interference is subject to improvement; however, it is felt to be sufficient for the present study. With these assumptions in mind, the wing theories used for load predictions are given in the following table:

Theories used for calculation of wing loads -		
Subsonic ($0.5 < M < 0.85$)	Transonic ($M = 1.0$)	Supersonic ($M \geq 1.2$)
All wings: linear lifting surface (refs. 1 to 4)	Swept wing: linear lifting surface (refs. 5 and 6) Unswept wing: two- dimensional flat plate; two- dimensional double wedge (refs. 7 and 8)	All wings: linear lifting surface (refs. 9 to 16)

In the subsonic range, for all wings, linear theory was applied. (See refs. 1 to 4.) These subsonic calculations were made up to a Mach number of 0.85, although in the neighborhood of this Mach number, transonic mixed-flow conditions no doubt exist. In the transonic range, calculations were made only for a free-stream Mach number of 1.0. In this range, for the swept wings, the linear theory presented by Mangler (ref. 5) which is in essence Jones' slender-wing theory (ref. 17) modified for linearized sonic-flow conditions was applied. For the unswept wing, at a Mach number of 1.0, use was made of the results of Guderley and Yoshihara (ref. 8) for a double-wedge section and the results of Guderley (ref. 7) for a flat plate of negligible thickness. For the supersonic Mach number range, the well-known lifting-surface theories were applied.

LOADING DISTRIBUTION

In the discussion of flight results, the chordwise and spanwise loadings for the unswept-wing X-1E airplane, the swept-wing D-558-II airplane, and the delta-wing JF-102A airplane are considered and then a force summary for all six airplanes is given.

Some idea of the flight Reynolds number, altitude, and angle-of-attack excursions for these airplanes can be determined from figure 2. The Reynolds number is given on a per-foot basis and for free-stream conditions. The open circular symbol represents the maximum Reynolds number obtained. It is noted that this flight Reynolds number varies from approximately 1×10^6 to 4×10^6 . The altitude covers a range from approximately 25,000 to 65,000 feet. On the right-hand side of figure 2 the hatched boundary is indicative of the maximum angle-of-attack excursions obtained in flight. The discussion of the angle-of-attack wing loads will be within the region shown by the dashed boundary.

In figures 3 to 6 are presented the chord loadings and span loadings for the X-1E wing panel. The solid line represents the theory; the open symbol, the flight data. The dashed line through the open circles represents "faired" flight data. The sketches on the left-hand side of figure 4 indicate the panel normal-force coefficient C_N for the angles of attack at which the chord and span loadings are shown. Consider first the chord loadings of figure 3, that is, the variation of ΔC_p , the lifting pressure, with x/c , the normalized distance from the leading edge. These results are for a span station $\frac{y}{b'/2} = 0.46$. The symbol b' denotes the external panel span. The chord loadings are shown for Mach numbers of 0.8, 1.0, and 1.9. For each Mach number the chord loadings are shown for two angles of attack, a low angle and a high angle. The magnitude of the high angle of attack is limited by the availability of the data. The angle of attack is always the angle of attack of the wing panel. At $M = 0.8$, the calculated level and variation of the chord loading compares favorably with the flight data. For a Mach number of 1.0, there is no available finite-span unswept-wing theory. The theoretical variation shown here is the flat-plate two-dimensional theory of Guderley. Although the level of the lifting pressure is not predicted herein, the variation is similar to the flight-measured variation for both angles of attack.

At supersonic speed and low angle of attack, the comparison of flight and theory is acceptable. At the higher angle of attack, the loading distribution is not predicted by theory although the level of the local load can be calculated. The midspan chord loadings and the chord loadings at two additional spanwise stations, one near the root and one near the tip, are shown in figures 5 and 6.

If the span-load distributions (fig. 4) are considered, it is noted that, at $M = 0.8$ and $M = 1.9$, the calculated span loading compares favorably with the flight-measured loading. For $M = 1.0$, the span loading was not calculated, since, as mentioned previously, the two-dimensional results of Guderley were used; however, the flight data have been faired. The shapes of the span-loading curves strongly resemble each other for the three Mach numbers shown.

For the swept-wing D-558-II airplane the chordwise and span-load distributions for the wing panel are shown in figures 7 to 10. The solid line represents the calculations and the open circular symbol, the flight measurements. The panel normal-force coefficients corresponding to the angles of attack considered are indicated in the sketches on the left-hand side of figure 8. The chord loadings presented in figure 7 are for a spanwise station close to the midsemispan location. For the subsonic and supersonic speeds, the theory allows the calculation of the level and variation of the chord loading except at the high angle of attack for the supersonic Mach number. At $M = 1.0$, the measured distribution of the lifting pressure ΔC_p is not calculated by the linear theory. Theory gives a zero loading behind the linearized sonic shock that starts from the leading edge of the streamwise tip of the wing panel. It is possible to obtain a nonzero loading by minor alterations of the wing-tip geometry so that, for the portion of the wing behind the linearized shock, the local span increases with increasing longitudinal position; and hence lift is produced. (See ref. 17.) A discussion of this artifice is given in the report by Mangler (ref. 5) mentioned earlier. The midspan chord loadings and the chord loadings near the root and tip are shown in figures 9 and 10.

The span loading for the swept-wing D-558-II is presented in figure 8. At subsonic and supersonic speeds the calculated distribution compares favorably with the flight measurements. For $M = 1.0$, the calculated loading, especially at the high angle of attack (11°), does not represent the experiment because of the inability of the theory to predict the level of the loads in the vicinity of the root and tip regions. At an angle of attack of 11° , the C_N of the panel is approximately 0.8. It is possible that separation effects at the root and tip are important for this configuration. In addition, the simple end-plate correction used herein for fuselage interferences may be approximate. In this regard the application of an analysis such as that reported by Crigler (ref. 6) for wing-body interference at sonic speeds would improve the prediction of the loading in the vicinity of the root.

The flight-measured loads for the wing panel of the 60° delta-wing JF-102A airplane are considered next. In figure 11 is shown an exploded view of the wing. Note the two fences located in the forward portion of

the wing and the elevon surface which is operative during flight. This wing has conical camber and a reflexed tip. For the calculation of the wing-panel loads, the effect of the fences and the effects of the conical camber and the reflexed tip are neglected; however, the effect of the elevon has been considered.

In figures 12 and 13 are shown the chord loading and the span loading for this airplane. For the lower angle-of-attack range (angles of attack from 3° to 5°) the calculations of the chord loadings compare favorably with the measurements. Up-elevon deflection is negative. The fact that the loading at the leading edge is not predicted is partly due to the omission of camber effect in the calculations. Although the effect of elevon at $M = 1.0$ was not calculated, an inspection of the low-angle-of-attack results indicates that the elevon load calculations at low supersonic speeds such as those obtained at $M = 1.2$ are reasonable approximations to the elevon load at $M = 1.0$. At the high angles of attack the remarks made for the low angles of attack for the sonic and supersonic Mach numbers are still reasonably valid. For the subsonic Mach number, the angle of attack is 20° and the calculations do not predict the flight measurement primarily because of leading-edge separation. For the case of leading-edge separation, calculations of the loading should be made within the framework of the approximate separation flow theories such as reported by Brown and Michael (ref. 18). The panel span loadings for the JF-102A are shown in figure 13. The inability of the calculations to produce the flight trends at $M = 0.8$ and $\alpha = 20^\circ$ is clear from the remarks relating to the chord loading at this Mach number and angle of attack. At $M = 1.0$, since the elevon load was neglected, the calculations overestimate slightly the level of the distribution. The effect of the fences on the span loading distribution can clearly be seen at $M = 1.0$ and $\alpha = 10^\circ$.

In general, the overall impression from this preliminary comparison is what would be expected from similar comparisons with wind-tunnel results. Briefly, a reasonable approximation of the span loadings can be determined for the low and moderate angle-of-attack range. The estimation of the chord loadings is less satisfactory, particularly in the neighborhood of a Mach number of 1.0.

NORMAL FORCES

In figure 14 is shown the variation of the panel normal-force coefficient with panel angle of attack. Note in this illustration that the open circular symbol represents the flight measurements for Mach numbers of 0.8 and 1.0. The solid symbol represents the flight measurements for supersonic Mach numbers. The calculations are again represented by the

solid lines. For the unswept wing at a Mach number of 1, the calculated variation is simply the result of Guderley and Yoshihara (ref. 8) for a two-dimensional wing with a 4-percent-thick double-wedge section. The theory here does not predict the magnitudes or the variation for the range of angle of attack where flight measurements are available. Tunnel results, however, for a similar wing indicate that the C_N variation with α is not linear and in the lower angle-of-attack range (below 4° angle of attack), theory more nearly agrees with the experimental variation.

In figure 15 an attempt has been made to show the effect of Mach number on the normal-force derivative C_{N_α} for all six airplanes that were sketched in figure 1. The theory is again represented by the solid line and, in addition, the inverted "V" symbol has been used to indicate the magnitude of C_{N_α} at $M = 1.0$. The flight data are represented by a square symbol. The solid symbol represents a low C_N range; the open symbol, a moderate C_N range; and the half-solid, a high C_N range. In most cases, flight data were available for only one of these ranges. For the X-1E at sonic speed, the difference in the calculated and flight values results from lack of flight data in the low C_N range as pointed out in the discussion of figure 14.

In general, the calculated normal-force-curve slopes compare favorably with those obtained from the flight data.

CONCLUDING REMARKS

In general, the overall impression from this preliminary comparison is what would be expected from similar comparisons with wind-tunnel results. Briefly, a reasonable approximation of the span loadings can be determined for the low and moderate angle-of-attack range. The estimation of the chord loadings is less satisfactory, particularly in the neighborhood of a Mach number of 1.0. In general, the calculated normal-force curve slopes compare favorably with those obtained from the flight data.

High-Speed Flight Station,
National Advisory Committee for Aeronautics,
Edwards, Calif., March 5, 1957.

REFERENCES

1. DeYoung, John, and Harper, Charles W.: Theoretical Symmetric Span Loading at Subsonic Speeds for Wings Having Arbitrary Plan Form. NACA Rep. 921, 1948.
2. DeYoung, John: Theoretical Symmetric Span Loading Due to Flap Deflection for Wings of Arbitrary Plan Form at Subsonic Speeds. NACA Rep. 1071, 1952. (Supersedes NACA TN 2278.)
3. Glauert, H.: The Elements of Aerofoil and Airscrew Theory. Second ed., Cambridge Univ. Press, 1947. (Reprinted 1948.)
4. Allen, H. Julian: Calculation of the Chordwise Load Distribution Over Airfoil Sections With Plain, Split, or Serially Hinged Trailing-Edge Flaps. NACA Rep. 634, 1938.
5. Mangler, K. W.: Calculation of the Pressure Distribution Over a Wing at Sonic Speeds. R. & M. No. 2888, British A.R.C., Sept. 1951.
6. Crigler, John L.: Comparison of Calculated and Experimental Load Distributions on Thin Wings at High Subsonic and Sonic Speeds. NACA TN 3941, 1957.
7. Guderley, Gottfried: The Flow Over a Flat Plate With a Small Angle of Attack at Mach Number 1. Jour. Aero. Sci., vol. 21, no. 4, Apr. 1954, pp. 261-274.
8. Guderley, Gottfried, and Yoshihara, Hideo: Two-Dimensional Unsymmetric Flow Patterns at Mach Number 1. Jour. Aero. Sci., vol. 20, no. 11, Nov. 1953, pp. 757-768.
9. Piland, Robert O.: Summary of the Theoretical Lift, Damping-in-Roll, and Center-of-Pressure Characteristics of Various Wing Plan Forms at Supersonic Speeds. NACA TN 1977, 1949.
10. Harmon, Sidney M., and Jeffreys, Isabella: Theoretical Lift and Damping in Roll of Thin Wings With Arbitrary Sweep and Taper at Supersonic Speeds - Supersonic Leading and Trailing Edges. NACA TN 2114, 1950.
11. Malvestuto, Frank S., Jr., Margolis, Kenneth, and Ribner, Herbert S.: Theoretical Lift and Damping in Roll at Supersonic Speeds of Thin Sweptback Tapered Wings With Streamwise Tips, Subsonic Leading Edges, and Supersonic Trailing Edges. NACA Rep. 970, 1950. (Supersedes NACA TN 1860.)

12. Tucker, Warren A., and Nelson, Robert L.: Theoretical Characteristics in Supersonic Flow of Two Types of Control Surfaces on Triangular Wings. NACA Rep. 939, 1949. (Supersedes NACA TN's 1600 and 1601 by Tucker and TN 1660 by Tucker and Nelson.)
13. Malvestuto, Frank S., Jr., and Hoover, Dorothy M.: Lift and Pitching Derivatives of Thin Sweptback Tapered Wings With Streamwise Tips and Subsonic Leading Edges at Supersonic Speeds. NACA TN 2294, 1951.
14. Hannah, Margery E., and Margolis, Kenneth: Span Load Distributions Resulting From Constant Angle of Attack, Steady Rolling Velocity, Steady Pitching Velocity, and Constant Vertical Acceleration for Tapered Sweptback Wings With Streamwise Tips - Subsonic Leading Edges and Supersonic Trailing Edges. NACA TN 2831, 1952.
15. Martin, John C., and Jeffreys, Isabella: Span Load Distributions Resulting From Angle of Attack, Rolling, and Pitching for Tapered Sweptback Wings With Streamwise Tips - Supersonic Leading and Trailing Edges. NACA TN 2643, 1952.
16. Martin, John C., Margolis, Kenneth, and Jeffreys, Isabella: Calculation of Lift and Pitching Moments Due to Angle of Attack and Steady Pitching Velocity at Supersonic Speeds for Thin Sweptback Tapered Wings With Streamwise Tips and Supersonic Leading and Trailing Edges. NACA TN 2699, 1952.
17. Jones, Robert T.: Properties of Low-Aspect-Ratio Pointed Wings at Speeds Below and Above the Speed of Sound. NACA Rep. 835, 1946. (Supersedes NACA TN 1032.)
18. Brown, Clinton E., and Michael, William H., Jr.: On Slender Delta Wings With Leading-Edge Separation. NACA TN 3430, 1955.

BIBLIOGRAPHY

- Banner, Richard D., Reed, Robert D., and Marcy, William L.: Wing-Load Measurements of the Bell X-5 Research Airplane at a Sweep Angle of 58.7° . NACA RM H55A11, 1955.
- Cole, J. D., Solomon, G. E., and Willmarth, W. W.: Transonic Flow Past Simple Bodies. (Contract AF 18(600)383; NAW-6154), GALCIT, 1953.
- Few, Albert G., Jr., and Fournier, Paul G.: Wind-Tunnel Investigation of the Aerodynamic Characteristics of a Series of Swept, Highly Tapered, Thin Wings at Transonic Speeds - Transonic-Bump Method. NACA RM L56I24, 1956.
- Heaslet, Max. A., and Fuller, Franklyn B.: Particular Solutions for Flows at Mach Number 1. NACA TN 3868, 1956.
- Heaslet, Max. A., and Spreiter, John R.: Three-Dimensional Transonic Flow Theory Applied to Slender Wings and Bodies. NACA TN 3717, 1956.
- Henderson, Arthur, Jr.: Wind-Tunnel Investigation of the Static Longitudinal and Lateral Stability of a 1/62-Scale Model of the X-1E at Supersonic Speeds. NACA RM L56C23b, 1956.
- Henderson, Arthur, Jr.: Wind-Tunnel Investigation of the Static Longitudinal and Lateral Stability of the Bell X-1A at Supersonic Speeds. NACA RM L55I23, 1955.
- Holder, D. W.: Note on the Flow Near the Tail of a Two-Dimensional Aerofoil Moving at a Free-Stream Mach Number Close to Unity. C.P. No. 188, British A.R.C., June 30, 1954.
- Keener, Earl R., and Jordan, Gareth H.: Wing Loads and Load Distributions Throughout the Lift Range of the Douglas X-3 Research Airplane at Transonic Speeds. NACA RM H56G13, 1956.
- Keener, Earl R., and Jordan, Gareth H.: Wing Pressure Distributions Over the Lift Range of the Convair XF-92A Delta-Wing Airplane at Subsonic and Transonic Speeds. NACA RM H55G07, 1955.
- Kuhl, Albert E., and Johnson, Clinton T.: Flight Measurements of Wing Loads on the Convair XF-92A Delta-Wing Airplane. NACA RM H55D12, 1955.
- Kuhn, Richard E., Hallissy, Joseph M., Jr., and Stone, Ralph W., Jr.: A Discussion of Recent Wind-Tunnel Studies Relating to the Problem of Estimating Vertical- and Horizontal-Tail Loads. NACA RM L55E16a, 1955.

- Lindsey, Walter F., and Johnston, Patrick J.: Some Observations on Maximum Pressure Rise Across Shocks Without Boundary-Layer Separation on Airfoils at Transonic Speeds. NACA TN 3820, 1956.
- Mayer, John P., and Hamer, Harold A.: A Study of Means for Rationalizing Airplane Design Loads. NACA RM L55E13a, 1955.
- Moseley, William C., Jr.: Investigation at Transonic Speeds of the Hinge-Moment Characteristics of a 1/8-Scale Model of the X-1E Aileron. NACA RM L55F06a, 1955.
- Neumark, S.: Critical Mach Numbers for Thin Untapered Swept Wings at Zero Incidence. R. & M. No. 2821, British A.R.C., Nov. 1949.
- Neumark, S., and Collingbourne, J.: Velocity Distribution on Thin Tapered Wings With Fore-and-Aft Symmetry and Spanwise Constant Thickness Ratio at Zero Incidence. R. & M. No. 2858, British A.R.C., June 1951.
- Nielsen, Jack N., Kaattari, George E., and Anastasio, Robert F.: A Method for Calculating the Lift and Center of Pressure of Wing-Body-Tail Combinations at Subsonic, Transonic, and Supersonic Speeds. NACA RM A53G08, 1953.
- Nielsen, Jack N., Spahr, J. Richard, and Centolanzi, Frank: Aerodynamics of Bodies, Wings, and Wing-Body Combinations at High Angles of Attack and Supersonic Speeds. NACA RM A55L13c, 1956.
- Polhamus, Edward C.: A Simple Method of Estimating the Subsonic Lift and Damping in Roll of Sweptback Wings. NACA TN 1862, 1949.
- Polhamus, Edward C.: Summary of Results Obtained by Transonic-Bump Method on Effects of Plan Form and Thickness on Lift and Drag Characteristics of Wings at Transonic Speeds. NACA TN 3469, 1955. (Supersedes NACA RM L51H30.)
- Robinson, Glenn H., Cothren, George E., Jr., and Pembo, Chris: Wing-Load Measurements at Supersonic Speeds of the Douglas D-558-II Research Airplane. NACA RM H54L27, 1955.
- Runckel, Jack F., and Gray, W. H.: An Investigation of Loads on Ailerons at Transonic Speeds. NACA RM L55E13, 1955.
- Shapiro, Ascher H.: The Dynamics and Thermodynamics of Compressible Fluid Flow. Vol. II. The Ronald Press Co., 1954.
- Spreiter, John R.: On the Application of Transonic Similarity Rules to Wings of Finite Span. NACA Rep. 1153, 1953. (Supersedes NACA TN 2726.)

- Spreiter, John R., and Alksne, Alberta: Theoretical Prediction of Pressure Distributions on Nonlifting Airfoils at High Subsonic Speeds. NACA Rep. 1217, 1955. (Supersedes NACA TN 3096.)
- Van Dyke, Milton D.: The Similarity Rules for Second-Order Subsonic and Supersonic Flow. NACA TN 3875, 1957.
- Vincenti, Walter G.: Measurements of the Effects of Finite Span on the Pressure Distribution Over Double-Wedge Wings at Mach Numbers Near Shock Attachment. NACA TN 3522, 1955.
- Vincenti, Walter G., Dugan, Duane W., and Phelps, E. Ray: An Experimental Study of the Lift and Pressure Distribution on a Double-Wedge Profile at Mach Numbers Near Shock Attachment. NACA TN 3225, 1954.
- Vincenti, Walter G., Wagoner, Cleo B., and Fisher, Newman H., Jr.: Calculations of the Flow Over an Inclined Flat Plate at Free-Stream Mach Number 1. NACA TN 3723, 1956.
- Vincenti, Walter G., and Fisher, Newman H., Jr.: Calculation of the Supersonic Pressure Distribution on a Single-Curved Tapered Wing in Regions Not Influenced by the Root or Tip. NACA TN 3499, 1955.
- Vincenti, Walter G., and Wagoner, Cleo B.: Theoretical Study of the Transonic Lift of a Double-Wedge Profile With Detached Bow Wave. NACA Rep. 1180, 1954. (Supersedes NACA TN 2832.)
- Vincenti, Walter G., and Wagoner, Cleo B.: Transonic Flow Past a Wedge Profile With Detached Bow Wave. NACA Rep. 1095, 1952. (Supersedes NACA TN's 2339 and 2588.)
- Willmarth, William W.: The Lift of Thin Airfoils at High Subsonic Speeds. OSR TN S4-168 (Contract AF-18(600)-383) GALCIT, June 1954.

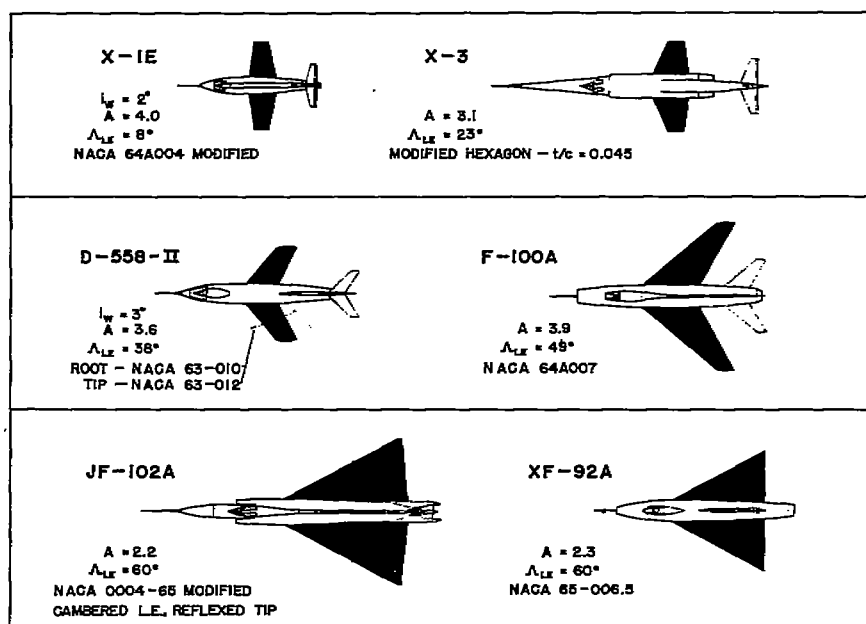


Figure 1

FLIGHT REYNOLDS NUMBER AND ANGLE OF ATTACK

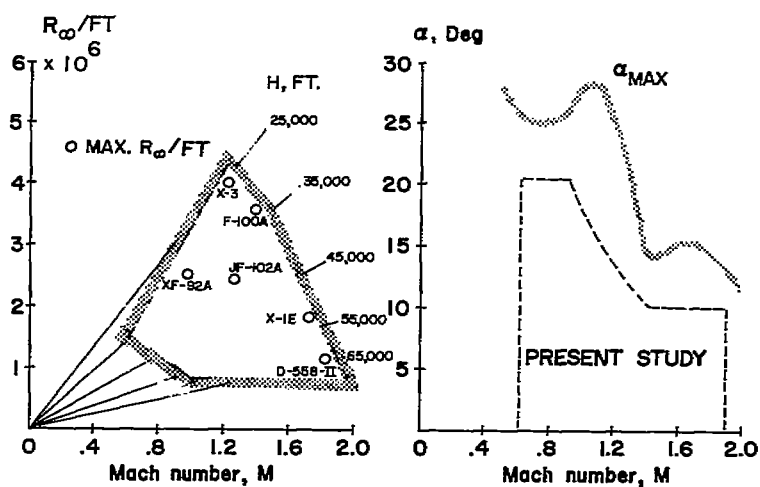


Figure 2

X-IE UNSWEPT WING. ($t/c = 0.04$) - CHORD LOADING
AT $y/b' / 2 = 0.46$

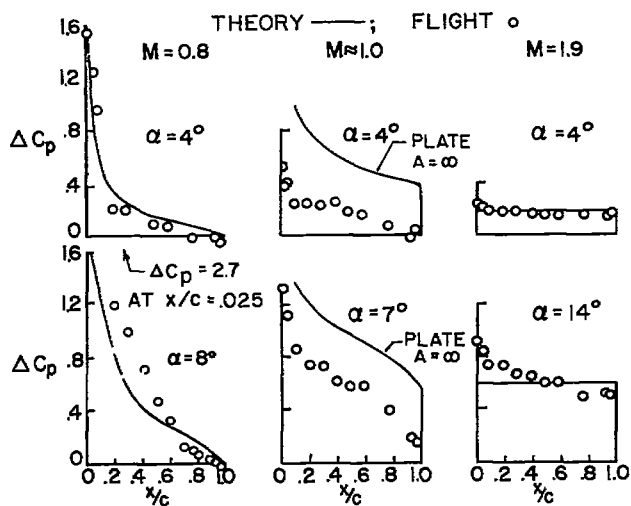


Figure 3

X-IE UNSWEPT WING ($t/c = 0.04$) SPAN LOADINGS
THEORY —; FLIGHT ○, ---○---

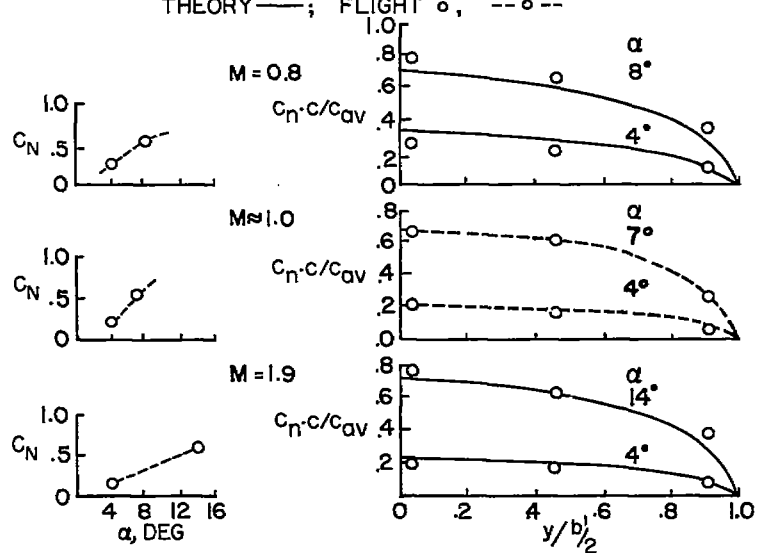


Figure 4

X-IE UNSWEPT WING-CHORD LOAD DISTRIBUTIONS
THEORY—, FLIGHT °

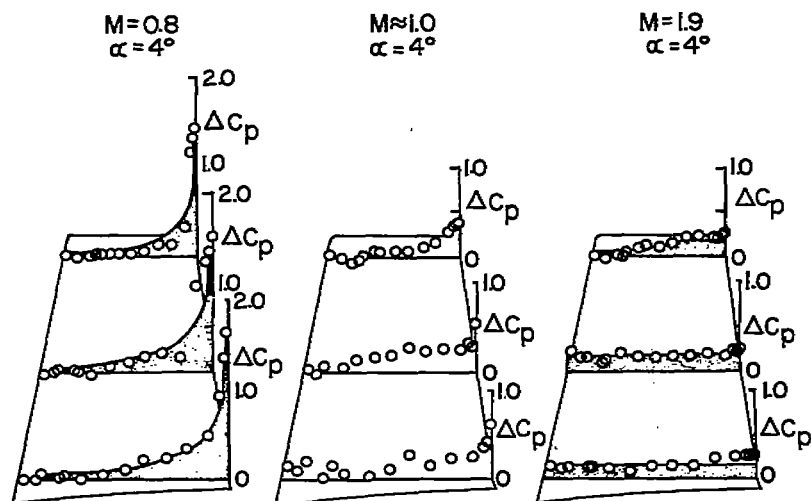


Figure 5

X-IE UNSWEPT WING-CHORD LOAD DISTRIBUTIONS
THEORY —, FLIGHT °

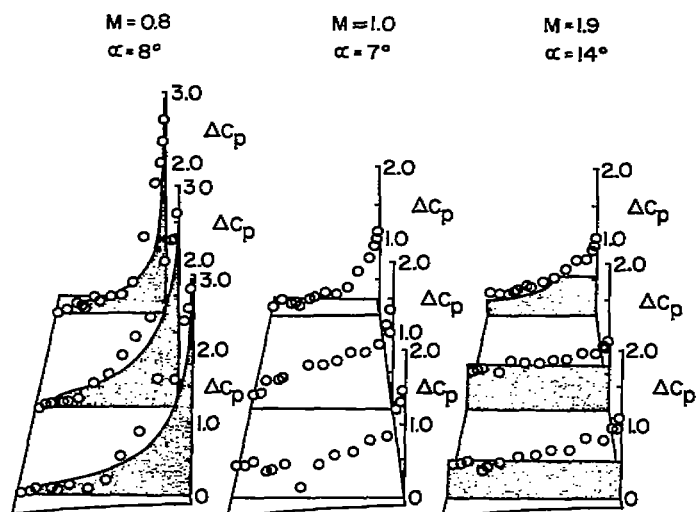


Figure 6

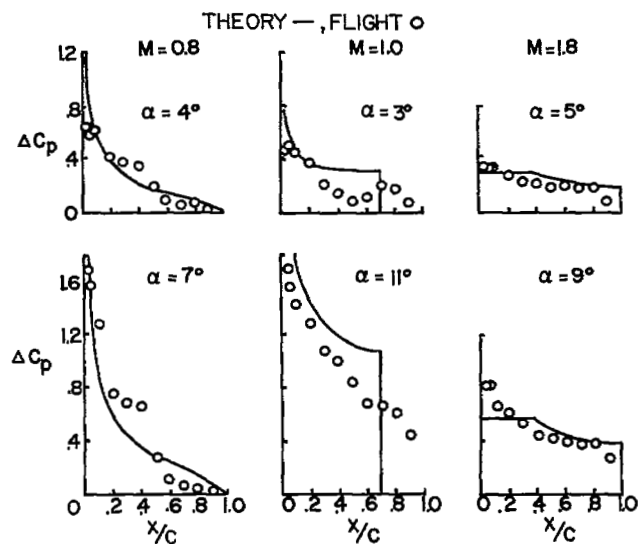
D-558-II SWEPT WING ($t/c \approx 0.09$)-CHORD LOADING AT $y/b_2 = 0.41$ 

Figure 7

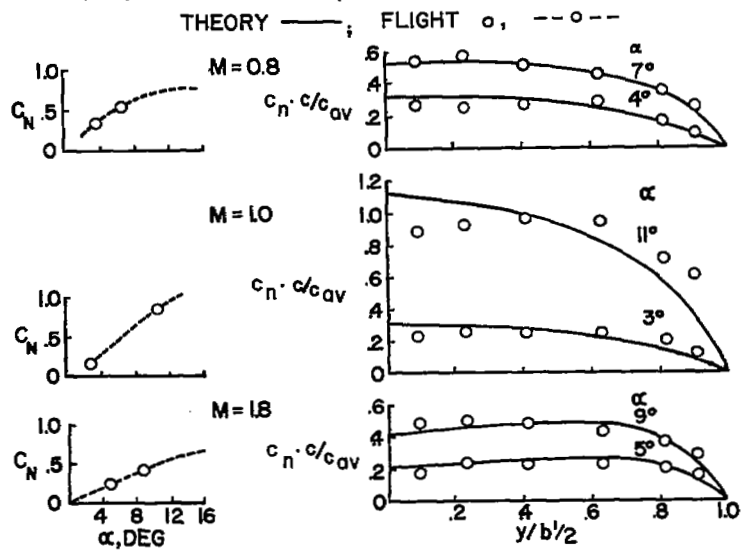
D-558-II SWEPT WING ($t/c \approx 0.09$) SPAN LOADINGS

Figure 8

D-558-II-SWEPT WING-CHORD LOAD DISTRIBUTIONS
THEORY—, FLIGHT ○

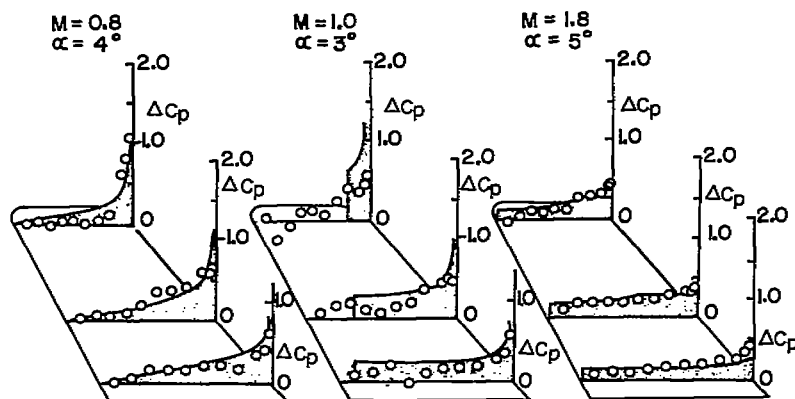


Figure 9

D-558-II SWEPT-WING CHORD LOAD DISTRIBUTION
THEORY—, FLIGHT ○

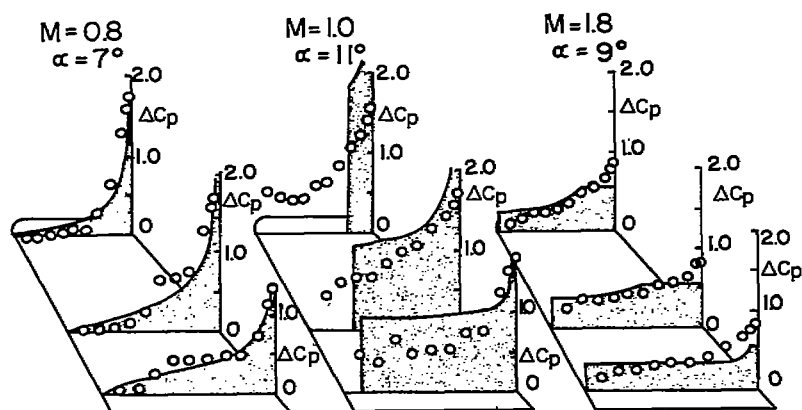
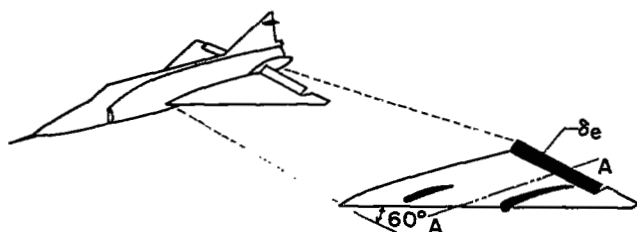


Figure 10

JF-102A AIRPLANE—SCHEMATIC OF WING



AT A-A, $c_f/c = 0.17$

$$b_f/b' = \frac{12.9}{16.2} = 0.795$$

Figure 11

JF-102A DELTA WING ($t/c=0.04$)—CHORD LOADING AT $y/b_2 = 0.34$
THEORY—(NO CAMBER), FLIGHT °

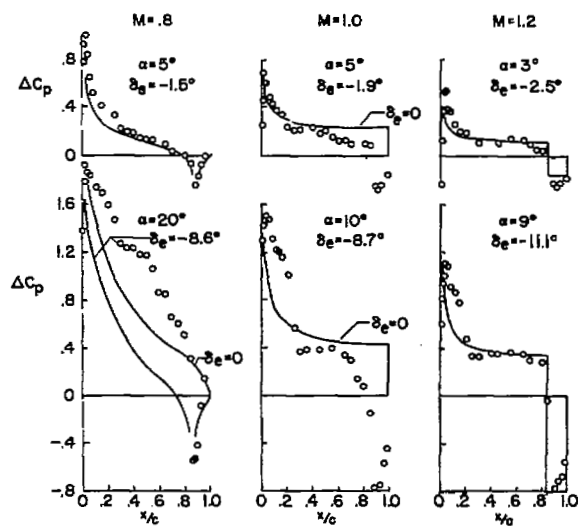


Figure 12

JF-102A DELTA WING ($t/c=0.04$) SPAN LOADINGS
THEORY —; FLIGHT \circ , -- \circ --

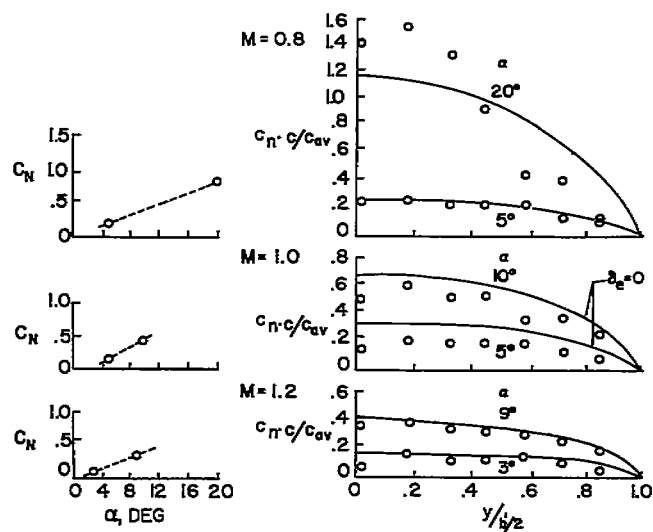


Figure 13

VARIATION OF NORMAL-FORCE COEFFICIENT WITH ANGLE OF ATTACK

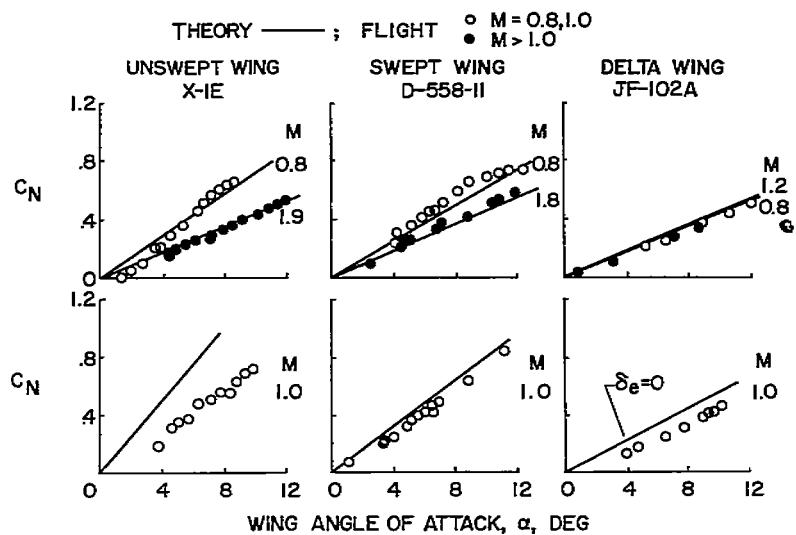


Figure 14

VARIATION OF FORCE COEFFICIENT DERIVATIVE WITH MACH NUMBER

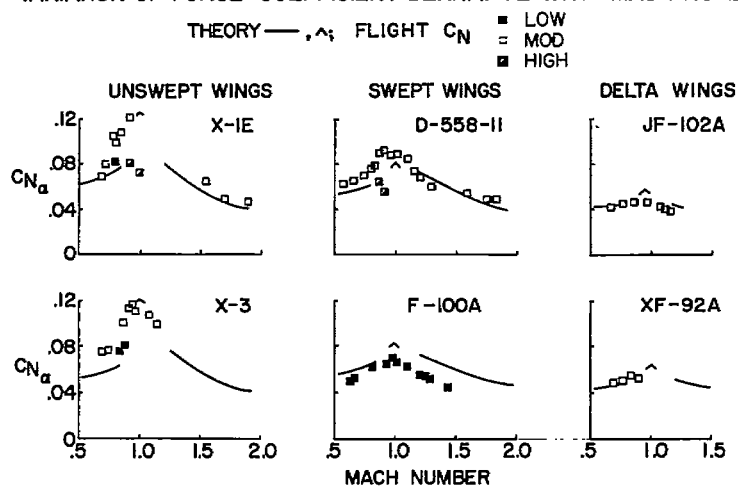


Figure 15